

Targeted Intracellular Delivery of Hydrophobic Agents using Mesoporous Hybrid Silica Nanoparticles as Carrier Systems

Jessica M. Rosenholm,^{†,||} Emilia Peuhu,^{‡,§,||} John E. Eriksson,^{‡,§}
Cecilia Sahlgren,^{*,‡,§,⊥} and Mika Lindén^{*,†,⊥}

Center for Functional Materials, Department of Physical Chemistry, Åbo Akademi University, Porthansgatan 3-5, FI-20500, Turku, Finland, Department of Biology, Åbo Akademi University, Artillerigatan 6A, FI-20520 Turku, Finland, and Turku Centre for Biotechnology, University of Turku and Åbo Akademi University, P.O. Box 123, FI-20521, Turku, Finland

Received May 19, 2009; Revised Manuscript Received June 9, 2009

ABSTRACT

Targeted nanoparticle-mediated intracellular delivery is demonstrated using two hydrophobic fluorophores as model drug cargo. The presented hybrid carrier system exhibits both cancer cell-targeting ability and capacity to retain a hydrophobic agent with subsequent specific release into the endosomal compartment. Furthermore, the incorporated agent is shown to be able to escape from the endosomes into the cytoplasm, making the particles promising candidates as carriers for targeted drug delivery for cancer treatment.

Targeted drug delivery is one of the key aims in medical sciences today. The application of nanotechnology in drug delivery has raised the expectations of achieving this goal and this field is likely to change the focus of the pharmaceutical and biotechnology industries in the future. By employing nanotechnology it may be possible to deliver, or even codeliver, drugs in a cell- and tissue specific manner. Targeting is especially relevant in the context of cancer therapies, as most of the commonly used anticancer drugs have serious side-effects due to unspecific action on healthy cells. Moreover, it is estimated that 40% or more of the active substances being identified by combinatorial screening programs are poorly soluble in water.¹ Poorly water-soluble compounds are difficult to develop as drug products using conventional formulation techniques,² and thus the hydrophobic character of such drugs make them interesting candidates for drug delivery systems. Many of the currently investigated nanotechnology approaches for the delivery of hydrophobic drugs rely on surfactant or polymer-related

formulations (see, for example, ref 3). However, cell specific targeting often remains a challenge.

Since the beginning of the millennium, much research has focused on applying mesoscopically ordered nanoporous silica materials as drug delivery systems,^{4–9} as these materials can carry a large amount of payload as a consequence of their high specific surface area and pore volume. Current efforts thus lie in introducing cell-specificity to these materials.^{9–11} However, successful intracellular delivery does not only require the drug delivery system to be internalized by the right population of cells, but also the ability of the system to release its cargo into the cytoplasm once taken up by the cell. Simultaneously, premature leaking of cargo before cellular internalization is not desirable. We have recently shown that poly(ethylene imine)-mesoporous silica hybrid particles could specifically target cancer cells under coculture conditions with normal cells using folic acid as the targeting ligand.¹¹ In the present study, the intracellular drug delivery ability combined with targetability of this system was verified using two hydrophobic fluorophores, DiI and DiO, as model drugs, which made it possible to follow the intracellular release by confocal fluorescence microscopy. Furthermore, the use of fluorophores as model cargo allows quantification of the intracellular delivery using flow cytometry.

* To whom correspondence should be addressed. E-mail: (C.S.) csahlgre@abo.fi; (M.L.) mlinden@abo.fi.

[†] Department of Physical Chemistry, Åbo Akademi University.

[‡] Department of Biology, Åbo Akademi University.

[§] Turku Centre for Biotechnology, University of Turku and Åbo Akademi University.

^{||} These authors contributed equally to this work.

[⊥] These authors contributed equally to this work.

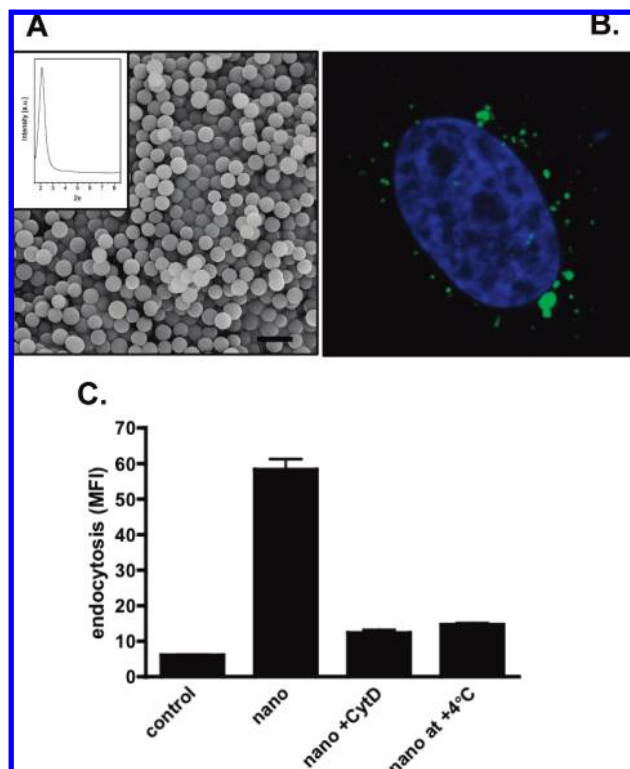


Figure 1. FA/PEI/FITC nanoparticles are actively endocytosed by cells. (A) X-ray diffraction analysis and SEM imaging of mesoporous silica nanoparticles. The scale-bar corresponds to 1 μm . (B) HeLa cervical carcinoma cells were cultured in DMEM medium supplemented with 10% fetal calf serum, 2 mM L-glutamin, 100 U/ml penicillin, 100 $\mu\text{g}/\text{mL}$ streptomycin in 37 $^{\circ}\text{C}$, 5% CO_2 . Nanoparticles were suspended in medium at a concentration of 10 $\mu\text{g}/\text{mL}$ and incubated with the cells for 24 h. The cells were fixed with 3% paraformaldehyde for 10 min and mounted with DAPI-Vectashield (Vector Laboratories) for nuclear labeling. Cells were viewed by Zeiss LSM 510 META laser-scanning confocal microscope (40 \times oil objective, 405/488 nm excitation, 3D projection). (C) HeLa cells were incubated for 3 h with 10 $\mu\text{g}/\text{mL}$ nanoparticles. To inhibit actin polymerization, the cells were pretreated with 10 μM cytochalasin D (CytD) for 30 min and incubated in 5 μM CytD during nanoparticle uptake. Alternatively, the cells were kept at +4 $^{\circ}\text{C}$ at all times. Intracellular FITC fluorescence (FL-1 channel) was analyzed by flow cytometry (FacsCalibur, BD Pharmingen) (Mean \pm SEM; $n = 3-5$).

Partially aminofunctionalized mesoporous silica nanoparticles with a mean diameter of about 300 nm were first synthesized using a mixture of aminotrimethoxysilane (APS) and tetramethoxysilane (TMOS) as the silica precursors and cetyltrimethylammonium chloride (CTACl) as the structure-directing agent, as previously described.^{11,12} An ethanolic FITC-solution was added in the synthesis step to create inherently fluorescent nanoparticles. Poly(ethylene imine), PEI (20 wt %), was grown onto the mesoporous silica particles by hyperbranching surface polymerization according to procedures described in our earlier publications.¹³ Folic acid was conjugated to the particles as described in ref 11.

The mesoscopic ordering of the pore system was verified by X-ray diffraction analysis, and the particle morphology was determined by scanning electron microscopy (SEM) (Figure 1A). A nanoparticle suspension was added to the cell media and incubated with the cells for 24 h. Confocal

microscopy analysis of the FITC fluorescence showed a dotted pattern of fluorescent particles indicating that the particles were located in intracellular vesicles (Figure 1B). We have previously shown by competition experiments using free folic acid that the preferential uptake mechanism of the folic acid-tagged particles by HeLa cells is by receptor-mediated endocytosis.¹¹ To further verify the active endocytosis mechanism, the uptake of nanoparticles was analyzed under conditions where cellular endocytosis was perturbed by incubating the cells at low temperatures or by inhibiting the dynamics of the actin cytoskeleton. To this end, cells were incubated at +4 $^{\circ}\text{C}$ or they were pretreated with cytochalasin-D, which specifically inhibits actin polymerization. Both methods of blocking endocytosis efficiently inhibited cellular uptake of particles, as demonstrated by flow cytometric analysis of intracellular FITC fluorescence (Figure 1C).

The potential of the system to deliver poorly water-soluble drugs to cells and the subsequent endosomal escape of the cargo was analyzed using particles loaded with lipophilic dyes. DiI (1,1'-dioctadecyl-3,3,3',3'-tetramethindocarbocyanine perchlorate) or DiO (3,3'-dioctadecyloxycarbocyanine perchlorate) dissolved in cyclohexane were loaded to a weight percent of one (1 wt %) into the mesoporous particles. No residual fluorophore remained in the supernatant after loading, as confirmed by UV-vis spectrophotometry (data not shown), indicative of quantitative loading. After vacuum drying overnight to remove any excess solvent, the particles were washed in a HEPES buffer solution (25 mM, pH 7.2) and resuspended in HEPES buffer at a concentration of 1 mg/mL. The particles were easily dispersible in HEPES, indicating that the amount of hydrophobic dye present on the outer surface of the particles was small.

Initially, the nanoparticles along with their cargo were compartmentalized in cellular vesicles, as demonstrated by highly overlapping green (FITC) and red fluorescence (DiI) (Figure 2A). However, after 24 h hours of incubation, a strong red coloration of the cellular body demonstrates successful release of DiI into the cytoplasm (Figure 2B), whereas the FITC labeled particles remained in the vesicular compartment. Importantly, fixation of cells led to an immediate endosomal escape of the dye, emphasizing the importance of performing the analysis of nanoparticulate intracellular delivery in live cells (Supporting Information; Figure 1).

DiI accumulates in lipid bilayers, including the membranes of cellular vesicles, and the dynamics of the vesicular trafficking in the cell in Figure 2B can be viewed in the video provided in the Supporting Information (Video 1). When the corresponding amount of DiI was added to the cell media without the carrier, very weak fluorescence was observed at 24 h (Figure 2B inset). This illustrates that intracellular delivery of DiI without a delivery system is not effective.

The release from the endosome-lysosome system might be assisted by the hyperbranched PEI grown on the particle surface. PEI has a buffering capacity at pH 4–6 and, hence, is able to destabilize endosomal membranes and

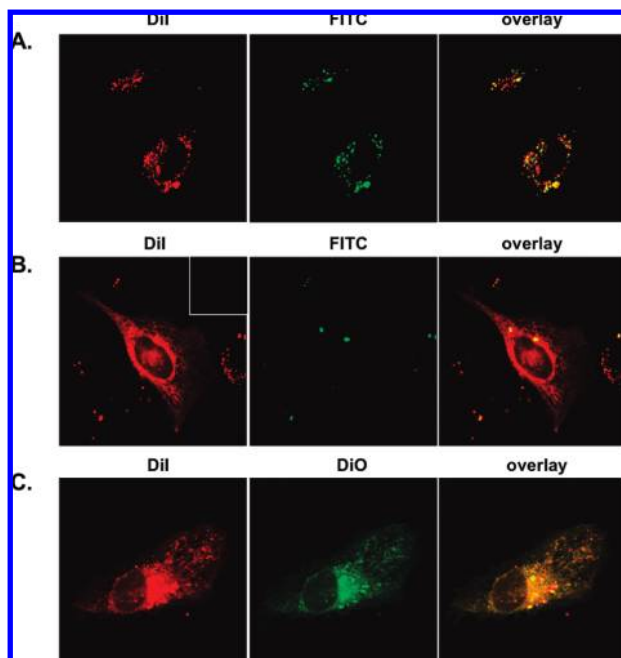


Figure 2. Codelivery and endosomal release of nanoparticle-loaded DiI and DiO inside the cell. HeLa cells were plated on glass-bottom culture dishes (MatTek Corp) and incubated with DiI-loaded (1 wt %) FA/PEI/FITC nanoparticles (10 $\mu\text{g}/\text{mL}$) for 24 h prior to analysis of live cells by confocal microscopy. (A) DiI (red channel) colocalizes initially with FITC-labeled (green channel) particles in endosomes. (B) In many cells, DiI can be seen released from the particle-containing endosomes to the cytoplasm. Corresponding amount of free DiI does not label the cells efficiently at 24 h of incubation (inset). (C) HeLa cells were incubated with DiI+DiO loaded (1 wt %) nanoparticles without FITC (10 $\mu\text{g}/\text{mL}$) for 24 h. DiI and DiO can be seen spreading with equal pattern inside the cell. All the images were taken with 40 \times oil objective and 488/545 nm excitation.

promote endosomal escape, which is a key to the successful application of PEI as an efficient gene transfection vector.¹⁴ In addition, folic acid-bound molecules have been shown to escape the endosomes after receptor-mediated endocytosis.¹⁵ Furthermore, the presence of FA has also been shown to enhance PEI-mediated transfection activity in serum.¹⁶ Thus, these particle modifications may have a synergistic effect on endosomal release following particle uptake. Furthermore, PEI may act as a molecular barrier inhibiting premature release before cell entry, as previously observed for mesoporous silica functionalized with polyamines.¹⁷

To investigate the specificity of the delivery, DiI was interchanged to the structurally very similar DiO, and the delivered amount was quantified by flow cytometry. As DiO fluoresces in green, the particles themselves were not FITC-labeled in this case. To verify the similar intracellular behavior of the two fluorophores, the nonfluorescent particles were first loaded with a total amount of 1 wt % DiI and DiO and the intracellular release in HeLa cells was followed (Figure 2C). The concurrent release of DiI and DiO demonstrates the possibility for efficient codelivery of two or more compounds. For quantification of targeted delivery to two different cell lines expressing different

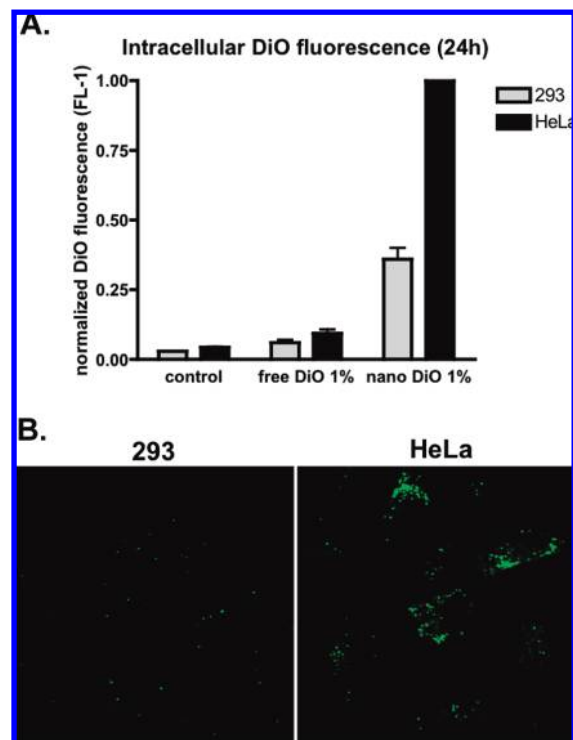


Figure 3. Nanoparticle-loaded DiO can be targeted to cancer cells. HeLa cells and HEK 293 (Human embryonic kidney; cultured as described in Figure 1) cells were incubated for 24 h with free 1% DiO or nonfluorescent FA/PEI nanoparticles (10 $\mu\text{g}/\text{mL}$) loaded with 1 wt % DiO. (A) Extracellular fluorescence was quenched by trypan blue and the intracellular DiO fluorescence was measured by flow cytometry. Mean fluorescence intensity of DiO (FL-1 channel) in other samples was normalized to HeLa cells incubated with nano DiO 1% (mean \pm SEM; $n = 4-6$). (B) Confocal microscope images of DiO fluorescence in live 293 and HeLa cells were taken after 24 h (40 \times oil objective, 488 nm excitation).

amounts of the folate receptor (FR), FA-tagged particles loaded with 1 wt % DiO were prepared. Cancerous HeLa (high FR) and epithelial HEK 293 (low FR) cells were incubated with the particles and the intracellular amount of DiO was analyzed by flow cytometry after 24 h. In order to detect only intracellular DiO, the extracellular portion of DiO was quenched by trypan blue prior to the analysis, as described in ref 11. HeLa cells had taken in considerably higher levels of DiO (Figure 3A), a result that was further confirmed by confocal microscopy. As seen in Figure 3B, extensive fluorescence was detected selectively in HeLa cells only. This experiment confirmed the selective delivery, and further demonstrated the superior efficiency of nanoparticle-mediated delivery, as compared to that of free hydrophobic agent. Furthermore, the release of DiI into the HEPES buffer was monitored by UV-vis spectrophotometry reading at $\lambda = 220.5$ nm. No leakage of DiI was observed within 24 h (data not shown). This suggests that premature leaking of the fluorescent agent during delivery does not occur in this case. This is also supported by the fact that no red fluorescence was detected in the cell membrane during the time of observation, suggesting that DiI remains inside the silica particles until being released inside the cell. The presented system, therefore, provides some interesting syn-

ergistic aspects in terms of endosomal release along with receptor-dependent targetability.

To conclude, we have successfully demonstrated targeted nanoparticle-mediated intracellular delivery of two hydrophobic fluorophores. The nanoparticles are taken up by receptor-mediated endocytosis followed by accumulation in the endosomal compartment and subsequent release of cargo into the interior of the cell. Thus, besides the selectivity of the developed nanoparticles for the cancer cells, the incorporated agent was shown to be able to escape from the endosomes into the cytoplasm, which is essential for successful intracellular delivery. In view of the hydrophobicity of many anticancer drugs, the presented carrier system, thus, constitutes a promising candidate for targeted drug delivery for cancer treatment.

Acknowledgment. Tommy Nyman is acknowledged for technical assistance. The financial support from the Academy of Finland Grants 128477 (E.P.) and 131034 (C.S.), the European Union (NanoEar project) (J.M.R.) and the partial financial support from the Tor, Joe, and Pentti Borg foundation are gratefully acknowledged.

Supporting Information Available: Paraformaldehyde fixation releases nanoparticle-delivered DiI from endosomes (Figure 1) and endosomal trafficking of cytoplasmic DiI (Video 1). This material is available free of charge via the Internet at <http://pubs.acs.org>.

References

- (1) Lipinski, C. *Am. Pharm. Rev.* **2002**, 5, 82–85.
- (2) Merisko-Liversidge, E.; Liversidge, G. G.; Cooper, E. R. *Eur. J. Pharm. Sci.* **2003**, 18, 113–120.
- (3) Merisko-Liversidge, E.; Liversidge, G. G. *Toxicol. Pathol.* **2008**, 36, 43–48.
- (4) Hartmann, M. *Chem. Mater.* **2005**, 17, 4577–4593.
- (5) Vallet-Regí, M.; Balas, F.; Arcos, D. *Angew. Chem., Int. Ed.* **2007**, 46, 7548–7558.
- (6) Trewyn, B. G.; Giri, S.; Slowing, I. I.; Lin, V. S.-Y. *Chem. Commun.* **2007**, 3236–3245.
- (7) Giri, S.; Trewyn, B. G.; Lin, V. S.-Y. *Nanomedicine* **2007**, 2, 99–111.
- (8) Slowing, I. I.; Trewyn, B. G.; Giri, S.; Lin, V. S.-Y. *Adv. Funct. Mater.* **2007**, 17, 1225–1236.
- (9) Slowing, I. I.; Vivero-Escoto, L.; Wu, C.-W.; Lin, V. S.-Y. *Adv. Drug Delivery Rev.* **2008**, 60, 1278–1288.
- (10) Liong, M.; Lu, J.; Kovochich, M.; Xia, T.; Ruhem, S. G.; Nel, A. E.; Tamanoi, F.; Zink, J. I. *ACS Nano* **2008**, 2, 889–896.
- (11) Rosenholm, J. M.; Meinander, A.; Peuhu, E.; Niemi, R.; Eriksson, J. E.; Sahlgren, C.; Lindén, M. *ACS Nano* **2009**, 3, 197–206.
- (12) Nakamura, T.; Yamada, Y.; Yano, K. *J. Mater. Chem.* **2007**, 17, 3726–3732.
- (13) (a) Rosenholm, J. M.; Penninkangas, A.; Lindén, M. *Chem. Commun.* **2006**, 37, 3909–3911. (b) Rosenholm, J. M.; Lindén, M. *Chem. Mater.* **2007**, 19, 5023–5034.
- (14) (a) Boussif, O.; Lezoualc'h, F.; Zanta, M. A.; Mergny, M. D.; Scherman, D.; Demeneix, B.; Behr, J. P. *Proc. Natl. Acad. Sci. U.S.A.* **1995**, 92, 7297–7301. (b) Godbey, W. T.; Wu, K. K.; Mikos, A. G. *J. Controlled Release* **1999**, 60, 149–160.
- (15) Betancourt, T.; Doiron, A.; Brannon-Peppas, L. In *Nanotechnology for Cancer Therapy*; Amiji, M. M., Ed.; CRC Press: Boca Raton, 2007; pp 215–30.
- (16) Guo, W.; Lee, R. J. *J. Controlled Release* **2001**, 77, 131–138.
- (17) (a) Casasús, R.; Marcos, MaD.; Martínez-Manez, R.; Ros-Lis, J. V.; Soto, J.; Villaescusa, L. A.; Amorós, P.; Beltran, D.; Guillem, C.; Latorre, J. *J. Am. Chem. Soc.* **2007**, 129, 8612–8613. (b) Casasús, R.; Climent, E.; Marcos, MaD.; Martínez-Mañez, R.; Sancenón, F.; Soto, J.; Amorós, P.; Cano, J.; Ruiz, E. *J. Am. Chem. Soc.* **2008**, 130, 1903–1917.

NL901589Y